Functional Ecology

British Ecological Society

Functional Ecology 2016 doi: 10.1111/1365-2435.12662

Nutrient utilization traits vary systematically with intraspecific cell size plasticity

Martino E. Malerba*[1,2,3], Kirsten Heimann[3,4] and Sean R. Connolly[3,5]

[1]*AIMS@JCU, James Cook University, Townsville, QLD 4811, Australia;* [2]*Australian Institute of Marine Science, Townsville, QLD 4811, Australia;* [3]*College of Marine and Environmental Sciences, James Cook University, Townsville, QLD 4811, Australia;* [4]*Centre for Sustainable Tropical Fisheries and Aquaculture, Townsville, QLD 4811, Australia; and* [5]*Australian Research Council Centre of Excellence for Coral Reef Studies, James Cook University, Townsville, QLD 4811, Australia*

Summary

1. Trait-based approaches are increasingly used to help understanding community structure and ecosystem functioning. A large proportion of trait-based studies define a species by its mean trait values and assume intraspecific trait variability to be negligible compared to interspecific differences. However, this assumption is rarely tested.

2. Phenotypic cell size plasticity can be particularly important in phytoplankton species, which are known for their rapid changes in cell size in response to variations in environmental conditions. While phytoplankton traits show clear systematic trends with mean cell size across species, how size-related plasticity influences the dynamics of a species remains unknown.

3. In this study, we evaluate the effects of cell size plasticity on the nitrogen (N) utilization traits of the green alga *Desmodesmus armatus* (Chlorophyta), reared in different inorganic nitrogen sources (nitrate, ammonium or both) and nutrient histories (N-replete and N-deplete).

4. Results show that traits for per-cell ammonium uptake, maximum cell growth rate and minimum N-quota change substantially within the study species, depending on mean cell size and nutrient history. In contrast, per-cell nitrate uptake was independent of cell size. These results indicate that representing phytoplankton species only by their mean trait values could underestimate the physiological performance of a species by as much as one order of magnitude.

5. This study highlights the extent to which explicit incorporation of within-species trait variability can enhance our understanding of how species performance changes along environmental gradients.

Key-words: allometric scaling, environmental gradients, green alga, intraspecific trait variability, kinetic parameters, nitrogen assimilation, observation error, process noise, process-based models, time series

Introduction

Explaining ecological communities and ecosystem functioning requires considering how multiple morphological and functional characteristics of a wide range of species change along various environmental gradients (McGill *et al.* 2006). Therefore, in ecology it is often advantageous to describe species not by their taxonomic identity, but rather by well-defined, measurable properties of a species that determine its performance ("functional traits"; McGill et al. 2006; Albert *et al.* 2010). When examining the distribution of a species and how it changes with biotic and abiotic factors, trait-based approaches allow far greater generality and predictability (e.g. plants with dense canopy are more temperature-tolerant) compared to more traditional nomenclature approaches focusing on species identities (e.g. species X grows better at temperature Y; Lavorel *et al.* 1997; Violle *et al.* 2007).

Ecological studies have often assumed that intraspecific variability in functional traits is negligible compared to interspecific differences (Albert et al. 2010; Albert *et al.* 2011). However, a growing number of studies report substantial intraspecific trait variability, challenging this assumption. For example, traits of subalpine grasslands and alpine meadows such as maximum height, leaf area and mass, and nitrogen and carbon concentrations display intraspecific variability with magnitudes of close to a third of interspecific variability (Albert et al. 2010). In some

*Correspondence author. E-mail: Martino.Malerba@my.jcu.edu.au

cases, intraspecific and interspecific trait variability are comparable in magnitude, such as for the leaf mass per area in the deciduous tree species *Nothofagus pumilio* compared to interspecific variation among northern hemisphere deciduous broad-leaved tree species (Fajardo & Piper 2011). Occasionally, intraspecific trait variability exceeds interspecific variability, such as for the seed size of pitcher plants in the genus *Sarraceniaceae* (Ellison 2001).

Intraspecific trait variability has the potential to be particularly important in phytoplankton ecology. Functional traits are commonly used to explain species trade-offs and optimal size, or size structure in phytoplankton communities (Grover 1990; Irwin *et al*. 2006; Litchman *et al*. 2007). Phytoplankton nitrogen utilization traits, such as the maximum uptake rate, the maximum growth rate and the ability to store nutrients, can be directly linked to the performance of the population, as well as its competitive ability within the community, and its contribution to nitrogen fluxes within the ecosystem (Falkowski, Barber & Smetacek 1998; Follows *et al*. 2007; Edwards *et al*. 2012). There is now considerable evidence showing that phytoplankton nutrient utilization traits change systematically with a species mean cell size (Chisholm 1992; Stolte & Riegman 1995; Litchman *et al*. 2007; Edwards *et al*. 2012). Specifically, small species show lower half-saturation constants for nutrient uptake (Litchman *et al*. 2007; Edwards *et al*. 2012) and higher population growth rates (but only for cell volumes >10 μm^3; Maranon *et al*. 2013), while large species show higher nutrient-uptake rates and greater ability to store nutrients (Stolte & Riegman 1996; Litchman & Klausmeier 2008; Edwards *et al*. 2012). However, phytoplankton cells are also known for displaying remarkable variations in cell size, as an indirect response to changes in environmental conditions (Duarte, Agusti & Canfield 1990; Dassow, Chepurnov & Armbrust 2006; Lyczkowski & Karp-Boss 2014). To our knowledge, no study has tested for the influence of intraspecific cell size plasticity on the population and nutrient-uptake dynamics of a species. If fluctuations in cell size were to substantially correlate with the physiological behaviour of a species, then characterizing phytoplankton trait distribution solely by interspecific allometric relationships is likely to underpredict a species' ability to respond and adjust to environmental fluctuations (Duarte, Agusti and Canfield 1990).

In this study, we test the hypothesis that changes in mean cell size are correlated with the nitrate-ammonium utilization dynamics of the widespread freshwater phytoplankton species *Desmodesmus armatus* (Chlorophyta). The nutrient utilization traits under analysis are: the per-capita uptake rates for nitrate and ammonium, the maximum cell growth rate and the minimum nitrogen quota. The experiment monitored the performance of the species under different nitrogen sources (nitrate, ammonium or both) and nutrient histories (N-replete and N-deplete). The effects of temporal changes in mean cell size, and of nutrient histories, on the nitrate-ammonium utilization of the species were evaluated by fitting dynamic models. Specifically, four alternative Quota-type models were designed and fitted to data by assuming different relationships between cell size and nutrient traits: (i) traits are independent of nutrient history and cell size ("baseline" model); (ii) traits depend only on nutrient history ("N-history" model), or (iii) only on cell size ("allometric" model); and (iv) traits depend on both cell size and nutrient history ("allometric N-history" model). Results show that the effects of cell size and N-history on nutrient utilization dynamics in *D. armatus* depend on the trait: ammonium uptake, maximum growth rate, and minimum internal N quota vary systematically with changes in cell size and previous N-history, while nitrate uptake is less related to both factors. This is the first study to quantify the importance of intraspecific trait variability on the population and nutrient-uptake dynamics of a species.

Materials and methods

PROCESS-BASED MODELS

Model presentation

The nitrate-ammonium-phytoplankton model proposed by Malerba, Connolly and Heimann (2015) was fitted to time series of *D. armatus* reared in laboratory conditions across treatments of nitrogen types (nitrate, ammonium, or both) and N-history (N-replete or N-deplete). The model followed the general assumptions of the original "Quota" model, first proposed by Droop (1974): cells take up nitrogen from the environment and divide at a cell-specific rate that is proportional to their internal nitrogen quota. Malerba, Connolly and Heimann (2015) extended this model to explicitly account for the dynamics of two specific types of nitrogen sources, with cells dividing after taking up either nitrate or ammonium or both. The main feature of the model is that phytoplankton cells can display different degrees of specialization towards ammonium or nitrate by presenting better kinetic parameters when reared with either source of nitrogen. Moreover, the model accounts for the interaction between nitrate and ammonium uptakes: high rates of ammonium uptake are known to repress nitrate uptake of a cell, by either altering the activity of specific transport enzymes or by preventing their synthesis (Syrett & Morris 1963; Berges 1997; L'Helguen, Maguer and Caradec 2008). The structure of the model was as follows (see Table 1 for definitions of state variables and parameters):

$$\frac{dNO_3}{dt} = -f_{NO_3}(NO_3(t)) \times f_{inhib}(NH_4(t)) \times B(t) \qquad \text{eqn 1a}$$

$$\frac{dNH_4}{dt} = -f_{NH_4}(NH_4(t)) \times B(t) \qquad \text{eqn 1b}$$

$$\frac{dQ}{dt} = [f_{NO_3}(NO_3(t)) \times f_{inhib}(NH_4(t)) + f_{NH_4}(NH_4(t))] - g(Q(t)) \times Q(t) \qquad \text{eqn 1c}$$

$$\frac{dB}{dt} = g(Q(t)) \times B(t) \qquad \text{eqn 1d}$$

with the four differential equations describing changes in nitrate ($NO_3(t)$), ammonium ($NH_4(t)$), internal cell nitrogen quota ($Q(t)$), and total population size ($B(t)$). The functional responses for $f_{NO_3}(NO_3(t))$ and $f_{NH_4}(NH_4(t))$ represent per-cell uptake of nitrate

and ammonium, respectively, with f_{inhib} ($NH_4(t)$) quantifying the inhibition of ammonium uptake on nitrate uptake. Finally, $g(Q(t))$ represents the functional response regulating the specific daily growth rate of a cell as a function of its internal nitrogen quota.

Traditionally, the per-capita nitrogen uptake rate of a cell is assumed to follow a saturable Michaelis-Menten functional response of the form $f_N = v_{\max} \times \frac{N(t)}{N(t)+k_N}$, where $v_{\max}$ is the maximum per-capita uptake rate and k_N is the half-saturation constant. However, preliminary analyses showed that the per-capita nitrogen uptake for the study species is linearly proportional to the nutrient concentration in the environment, for the range of concentrations considered here (see Appendix S1 in Supporting information). A linear functional response for per-cell nitrogen uptake is consistent with physiological studies. Phytoplankton cells have evolved two alternative uptake systems to better cope with fluctuating nutrient availabilities (Collos *et al.* 1997; Flynn 1999; Collos, Vaquer & Souchu 2005). High nutrient concentrations (~100–1000 μmol-N L^{-1}) induce the expression of a low-affinity system, which is linearly proportional to external nitrogen (Crawford *et al.* 2000). Conversely, low nutrient concentrations (1–100 μmol-N L^{-1}) induce a high-affinity system, which follows a saturable function of external nitrogen concentration (Crawford *et al.* 2000). Hence, per-cell nitrate and ammonium uptake rates were modelled as a linear functional of medium nitrogen:

$$f_{NO_3}(NO_3(t)) = w_{NO_3} \times NO_3(t) \qquad \text{eqn 2a}$$

$$f_{NH_4}(NH_4(t)) = w_{NH_4} \times NH_4(t) \qquad \text{eqn 2b}$$

where w_{NO_3} and w_{NH_4} are the per-cell nitrate and ammonium uptake rates respectively (units of $cell^{-1}$ day^{-1}).

Physiological studies have shown that ammonium inhibition on nitrate uptake depends on the per-cell ammonium uptake rate (not on the external ammonium concentration; Syrett & Morris 1963). The specific form of this functional response can depend on the species and the experimental conditions, ranging from an immediate cessation of nitrate utilization in the presence of ammonium, to a less abrupt transition, or even to the absence of any interactions between ammonium and nitrate uptake. A general and flexible way to parameterize the effect of ammonium inhibition on nitrate uptake is using a negative exponential functional response between 0 (fully inhibited) and 1 (no inhibition), as:

$$f_{\text{inhib}}(NH_4(t)) = e^{-a \times f_{NH_4}(NH_4(t))^b} \qquad \text{eqn 3}$$

with a and b regulating the shape of the curve.

Finally, the function $g(Q)$ regulates the growth rate of a cell as a function of its internal nitrogen quota. For phytoplankton species, this relationship is commonly represented with a nonlinear rectangular hyperbola of the form:

$$g(Q(t)) = \mu_{\text{inf}} \times \left(1 - \frac{Q_{\min}}{Q(t)}\right) \qquad \text{eqn 4}$$

where μ_{inf} indicates the growth rate at infinite internal quota and $Q_{\min}$ indicates the concentration of per-cell internal nitrogen quota at which no cell division occurs (with $Q(t) \geq Q_{\min}$).

Alternative models

Four alternative models were derived assuming different functional responses for describing the traits for the species. The first model ("baseline model") assumes that all traits in eqns 2a–b and 4 (i.e. w_{NO_3}, w_{NH_4}, μ_{inf} and $Q_{\min}$) are fixed species-specific terms. The second model ("N-history model") instead assumes that the traits of the species differ with previous nitrogen history. Empirical studies have documented that N-deplete cells often respond to new nitrogen availability with transient rates of higher nitrogen uptake and lower cell growth rates (Cochlan & Harrison 1991; Sinclair *et al.* 2006). Hence, this model includes two independent sets of parameters to describe the species' traits for nitrogen

Table 1. Best-estimates from the posterior distribution (median and upper and lower 95% credible intervals) of the parameters in the "allometric N-history" model, which was the best-fitting model following DIC model selection (confront to Table 2 for DIC scores). Parameter values were calculated using observation error-only likelihood function

State variables	Definition (units)
NO_3	Nitrate in medium (μmol NO_3^- L^{-1})
NH_4	Ammonium in medium (μmol NH_4^+ L^{-1})
Q	Nitrogen quota (μmol N $cell^{-1}$)
B	Population density ($cell$ L^{-1})
Parameters	**Definition [Median (± 95% CI) units]**
w_{NO_3}_coef_rep	Scaling intercept for per-cell nitrate uptake in replete cells [6·76 (5·81–7·81) 10^{-10} $cell^{-1}$ cell $area^{-1}$ day^{-1}]
w_{NO_3}_exp_rep	Scaling exponent for the per-cell nitrate uptake in replete cells [2·55 (0–3·69) 10^{-6} unitless]
w_{NH_4}_coef_rep	Scaling intercept for the per-cell ammonium uptake in replete cells [2·44 (0·38–79·3) 10^{-16} $cell^{-1}$ cell $area^{-1}$ day^{-1}]
w_{NH_4}_exp_rep	Scaling exponent for the per-cell ammonium uptake in replete cells [4·64 (3·5–6) unitless]
μ_{inf}_coef_rep	Scaling intercept for growth rate at infinite nutrient quota in replete cells [4·09 (1·18–19·2) 10^{-5} day^{-1} cell $area^{-1}$]
μ_{inf}_exp_rep	Scaling exponent for growth rate at infinite nutrient quota in replete cells [3·2 (2·7–3·6) unitless]
$Q_{\min}$_coef_rep	Scaling intercept for per-cell minimum nitrogen quota in replete cells [5·93 (1·65–7·8) 10^{-8} μmol N $cell^{-1}$ cell $area^{-1}$]
$Q_{\min}$_exp_rep	Scaling exponent for per-cell minimum nitrogen quota in replete cells [7·79 (0·04–53·9) 10^{-2} unitless]
w_{NO_3}_coef_dep	Scaling intercept for the per-cell nitrate uptake in deplete cells [11·9 (9·98–14·6) 10^{-10} $cell^{-1}$ cell $area^{-1}$ day^{-1}]
w_{NO_3}_exp_dep	Scaling exponent for the per-cell nitrate uptake in deplete cells [10·9 (0–13·9) 10^{-8} unitless]
w_{NH_4}_coef_dep	Scaling intercept for the per-cell ammonium uptake in deplete cells [4·43 (1·6–12·9) 10^{-12} $cell^{-1}$ cell $area^{-1}$ day^{-1}]
w_{NH_4}_exp_dep	Scaling exponent for the per-cell ammonium uptake in deplete cells [1·83 (1·49–2·15) unitless]
μ_{inf}_coef_dep	Scaling intercept for growth rate at infinite nutrient quota in deplete cells [0·49 (0·33–0·72) day^{-1} cell $area^{-1}$]
μ_{inf}_exp_dep	Scaling exponent for growth rate at infinite nutrient quota in deplete cells [0·3 (0·16–0·43) unitless]
$Q_{\min}$_coef_dep	Scaling intercept for per-cell minimum nitrogen quota in deplete cells [5·56 (4·13–7·53) 10^{-10} μmol N $cell^{-1}$ cell $area^{-1}$]
$Q_{\min}$_exp_dep	Scaling exponent for per-cell minimum nitrogen quota in deplete cells [1·89 (1·78–2·01) unitless]
a	Shape parameters for the inhibition of ammonium uptake on per-cell nitrate uptake [1·05 (0·1–13·9) 10^{-4} unitless]
b	Shape parameters for the inhibition of ammonium uptake on per-cell nitrate uptake [0·55 (0·4–0·71) unitless]

uptake and growth rate: one to represent experiments whose inoculum was previously N-replete ($w_{NO_3\_rep}$,$w_{NH_4\_rep}$, μ_{inf_rep}, Q_{min_rep}) and another for experiments whose inoculum was N-deplete ($w_{NO_3\_dep}$, $w_{NH_4\_dep}$, μ_{inf_dep}, Q_{min_dep}). Overall, the "N-history" model included eight estimated demographic parameters. The third alternative model ("allometric model") assumed that N-utilization traits of a species are a power-law function of the mean cell size in the population. For example, the trait for the nitrate uptake rate of a cell now becomes:

$$w_{NO_3}(\text{size}(t)) = w_{NO_3\_coef} \times \text{size}(t)^{w_{NO_3\_exp}} \quad \text{eqn 5}$$

with size(t) as the area (unit: μm^2) of a cell at time t, $w_{NO_3\_coef}$ and $w_{NO_3\_exp}$ as tuneable demographic parameters regulating the shape of the relationship. In this way, each demographic parameter in the "baseline model" became an allometric function of cell size, for a total of eight estimated parameters. Because there is strong biological evidence indicating that phytoplankton cells uptake nitrogen at a rate that is proportional to their cell surface area (Aksnes & Egge 1991), both $w_{NO_3\_exp}$ and $w_{NH_4\_exp}$ were constrained to be positive. Also Q_{min_exp} was constrained to be positive, as the minimum internal nitrogen quota of a cell is directly proportional to the cell area (Shuter 1978; Edwards *et al*. 2012). We also checked that removing these constraints did not change the interpretation of the results. Notice that the slope between the size and the maximum growth rate of a cell was left unconstrained, as this relationship can either be positive or negative depending on the mean cell size of the species (Wirtz 2011; Maranon *et al*. 2013). Finally, the fourth "allometric N-history" model merges the assumptions of the "allometric model" and the "N-history" model: each trait in the "N-history" model follows an allometric function of mean population cell size. Hence, this parameterization assumes that the effect of cell size changes depending on whether the inoculum was N-replete or N-deplete before the experiment, with a total of 16 estimated demographic parameters.

It is biologically possible that the ammonium inhibition on the nitrate uptake of a cell is also influenced by size and N-history. However, there was not enough information in the data to calibrate size- or N-history-dependent functional responses for eqn 3.

DATA COLLECTION

Culture maintenance

Monoclonal 1·2 L batch cultures of the green microalga *D. armatus* (R. Chod.) Hegev. (culture accession: NQAIF301, sourced from the North Queensland Algal Culturing and Identification Facility at James Cook University, Townsville, QLD) were reared in standard Bold Basal Medium (BBM; Nichols 1973). Cultures were kept in a temperature-controlled room at 27 ± 3°C with a 14–10 day-night cycle at a light intensity of 70 μmol photons m^{-2} s^{-1}. Nitrogen was set as the limiting factor for growth in all experimental cultures, supplied between 4 to 8 times below the recommended BBM concentration with either sodium nitrate ($NaNO_3$) for nitrate-BBM, or ammonium chloride (NH_4Cl) for ammonium-BBM, or both. Phosphorous, iron and all other nutrients were supplied at non-limiting concentrations (see Appendix S2 for more details on laboratory protocols).

Experimental design

The experimental set-up was a factorial design of two treatments of cell N-history (N-replete and N-deplete) crossed with three treatments of nitrogen type (nitrate, ammonium or both), each replicated with three 1·2 L independent replicate cultures (see Appendix S3 for experimental design). Initial medium nitrogen was standardized to 800 μM-N. The initial population density in the experimental cultures was standardized at 1×10^9 cells mL^{-1}, which ensured between 4 to 8 days of rapid growth before reaching stable population densities. For N-replete cultures, exponentially growing cells were taken from a mother culture and inoculated into experimental cultures with fresh N-rich BBM medium. Data collection started immediately after inoculation. For N-deplete cultures, exponentially growing cells from the mother culture were inoculated into experimental cultures with N-free BBM medium. Cells were monitored until population density reached stationary growth, to ensure that all internal nitrogen quota was consumed before the beginning of the experiment (typically 3–4 days). Data collection started following fertilization of the N-free medium with nitrogen.

Data collection for population density, mean cell size and medium nitrogen

Three replicate measurements per culture were taken every day by loading 250 μL on a 96 well plate and measured with a Guava EasyCyte flow cytometer (Millipore, Hayward, CA, USA). To control for the effects of the 14–10 day-night photoperiod cycle on cell cycle, data collection was conducted daily at 13:00 (7 h into the light period). Before cytometric analysis, each sample was diluted with DI water between 25 and 50 times to maintain the optimal precision range of the instrument (50–500 cells μL^{-1}). Population size was estimated after excluding dead cells and inorganic particles characterized by low red fluorescence signals. Mean cell size was estimated optically through the forward light scatter recorded with the flow cytometer. Mullaney, Dilla and Coulter (1969) showed that the light refraction at small angles (i.e. forward light scatter) was proportional to the size of the particle, as predicted by Mie theory (Sharpless *et al*. 1975; Sharpless & Melamed 1976; Veldhuis & Kraay 2000; Shapiro 2005). Light microscopy validated the use of forward light scatter as an accurate linear proxy for mean cell size (cell area: $F_{1,\ 17} = 64{\cdot}9$, $P < 0{\cdot}001$, $R^2 = 0{\cdot}79$; cell perimeter: $F_{1,\ 17} = 49{\cdot}6$, $P < 0{\cdot}001$, $R^2 = 0{\cdot}66$; see Appendix S4). Instrument precision was periodically checked with Guava easyCheck beads (Catalog No. 4500-0025; Millipore), ensuring a coefficient of variation (CV) <5% for all detectors. Medium nitrogen concentration was quantified using standard laboratory protocols: the ultraviolet spectrometric screening method for nitrate (NO_3^-; Collos *et al*. 1999; Lanoul, Coleman & Asher 2002; Malerba, Connolly & Heimann 2016a), and the salicylate–hypochlorite method for ammonium concentrations (Bower & Holm-Hansen 1980; please refer to Appendix S2 for more details on laboratory protocols).

MODEL CALIBRATION

We fitted the four process-based models to data for medium nitrogen and population density from all experiments. This way, model predictions generated from a single set of parameters were confronted with time series from six different combinations of nitrogen types and N-histories, with each treatment replicated three times. Quota dynamics were not experimentally measured but were instead inferred from the model fits: all of the parameters that influence the dynamics of the unobserved internal quota ($Q(t)$) also appear in the equations for the observed dynamics for nitrate depletion and biomass growth. Hence, flux into the quota can be inferred from changes in medium nitrate and ammonium, while flux out of the quota can be inferred from changes in population density (De La Rocha *et al*. 2010; Malerba, Connolly & Heimann 2012; Malerba, Connolly and Heimann 2015).

Two different sources of error can affect parameter calibration from time-series data: observation error and process noise

(Hilborn & Mangel 1997; Bolker 2008). Observation error refers to unexplained variation caused by instrumental error, while process noise refers to unexplained variation due to natural stochasticity in the culture dynamics. While highly controlled experimental systems are typically more consistent with process noise (Bolker 2008), the use of an optical proxy for mean cell size has the potential to increase the effects of observation error. Therefore, we adopted in this study the common approach of fitting two separate likelihood functions, one accounting for process error-only and a second one for observation error-only (see Malerba, Connolly and Heimann 2012 for a detailed description and justification of the likelihood functions for Quota models). We then checked that model selection and parameter estimation gave comparable results for the two methods, and supported the same conclusions. Markov Chain Monte Carlo techniques, with Adaptive Mixture-Metropolis and Random Walk Metropolis and uniform priors, were used to fit all models, using package LaplacesDemon (Hall 2008) in the software R (R Core Team 2015). To monitor for successful convergence, we visually inspected the iterated history, density plot and correlation diagram for each of the parameters on four chains, and we checked for a potential scale reduction factor lower than 1·2 using Gelman and Rubin's MCMC convergence diagnostic (Gelman & Rubin 1992).

MODEL SELECTION

The goodness-of-fit for the "Baseline", "N-history", "Allometric" and "Allometric N-history" models were compared using Deviance Information Criteria (DIC), which with uninformative prior distribution of the parameters approaches $D(\theta) + 2 \times k$, where $D(\theta)$ is the mean of the posterior distribution for the deviance and k is the total number of calibrated parameters (Spiegelhalter *et al*. 2002; Hooten & Hobbs 2015). The model with the lowest DIC score is the estimated best-fitting model. In general, models separated by more than 5–10 DIC units from the best model should be considered as fitting the data substantially worse (Spiegelhalter *et al*. 2002). Model goodness-of-fit was also evaluated in two additional ways. Specifically, we calculated a standard coefficient of determination (R^2) for each state variable in each experiment, and we also inspected the distribution of residuals around predicted values.

PHENOMENOLOGICAL MODELS

The main advantage of fitting process-based models to our data is that it allows calibrating species-specific functional responses on data from all variables at once, thereby quantifying how flows of nitrogen among ambient nitrate and ammonium, internal nitrogen quota and population density influence one another. However, most published demographic parameters for phytoplankton species have not been calculated in this way, but rather by calibrating each functional response independently, using more traditional least-squared regression between successive points in time of each individual variable. Hence, we also tested if the conclusions from our dynamic model analysis were consistent with least-squared regressions from observed rates of per-cell nitrate and ammonium uptake and cell growth rate (see Appendix S5).

Results

The "Allometric N-history" model was selected as the best-fitting model by DIC model selection (Table 2). This model assumes that the species traits follow two different allometric relationships with cell size, depending on the N-history of the cell. The "Baseline" model, which assumes that all demographic parameters are independent of cell size and N history, performed the worst (Table 2). The "Allometry" model, which assumes that demographic parameters vary with cell size, and the "N-history" model, assuming N-replete and N-deplete cells to display different size-independent demographic parameters, ranked in-between (Table 2). Furthermore, calibrating the model with either observation error-only or process noise-only likelihood functions produced equivalent conclusions, which indicates that the results are robust and independent of the assumptions about the source of error in the data (Table 2). Finally, these results were also consistent with phenomenological models of observed rates of nitrate and ammonium utilization using least-squared regression (see Appendix S5).

Except for the rates of per-cell nitrate uptake, all species traits show substantial differences when estimated with the "Allometric N-history" model (solid lines) compared to the size- and N-history-independent "Baseline" model (dashed lines; Fig. 1). Specifically, per-cell ammonium uptake was substantially influenced by mean cell size, and was higher in N-deplete cells than N-replete cells (Fig. 1b). The maximum specific growth rate increased with cell size for N-replete cells, but remained approximately constant for N-deplete cells (Fig. 1c). Finally, minimum internal nitrogen quota was an increasing function of cell size for N-deplete cells, while was independent of size for N-replete cells (Fig. 1d). Conversely, per-cell nitrate uptake was independent of cell size and was comparable between N-replete and N-deplete cells (Fig. 1a). Functional responses calibrated by fitting the model with observation error-only

Table 2. Formal model selection criteria between competing models with Deviance Information Criterion (DIC). Values represent the total number of estimated parameters (Pars), mean deviance (D(θ)), the DIC score and the difference in DIC (ΔDIC) scores (thus, by definition, the best fit model has ΔDIC = 0), for models calibrated with either observation error-only or process noise-only likelihood functions. Boldface indicates the model with greater support from the data.

	Observation error				Process error			
Alternative models	Pars	D(θ)	DIC	ΔDIC	Pars	D(θ)	DIC	ΔDIC
Allometry N-History	49	29 527	29 571	0	35	9898	9928	0
N-History	41	30 004	30 044	474	27	10 007	10 029	101
Allometry	41	30 034	30 078	508	27	10 106	10 131	203
Baseline	37	30 212	30 249	678	23	10 138	10 165	238

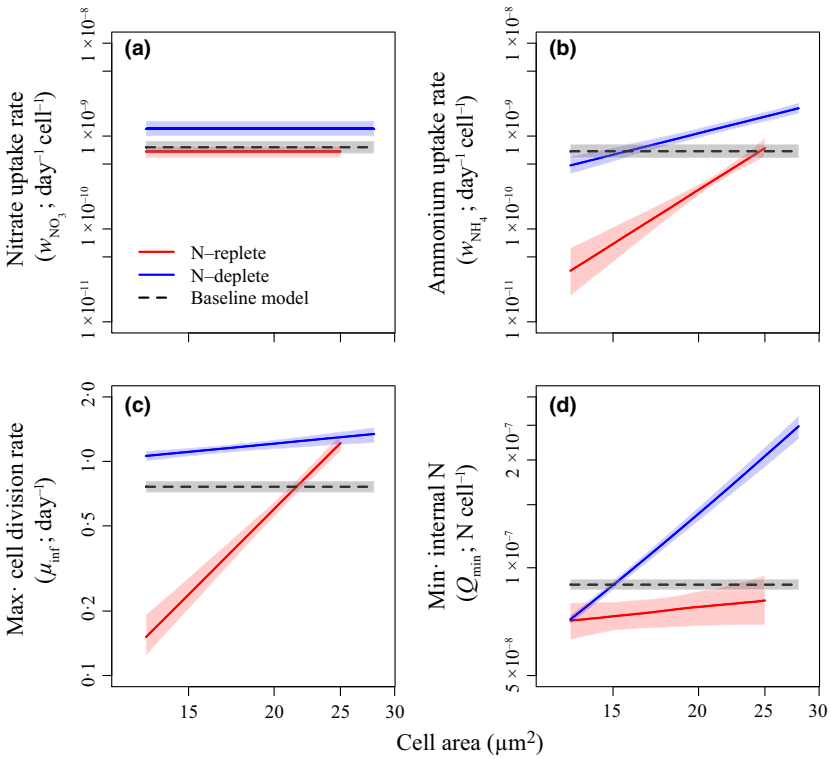

Fig. 1. Comparison for the best-estimates for demographic parameters (median ±95% credible intervals) calculated with the "baseline" model (dashed lines) and with the best-fitting "Allometric N-history" model (solid lines). Parameters were calculated using observation error-only likelihood functions and represent rate of per-cell uptake for nitrate (a) and ammonium (b), growth rate at infinite stored internal nitrogen quota (c), and minimum internal nitrogen quota (d). Two solid lines in the same pannel represent the effect of cell size on the demographic parameters between N-replete (red) and N-deplete (blue) previous N-history. Dashed line is the corresponsive parameter estimated with the "baseline" model, which assumes independence with cell size and nutrient history. See Material and Methods, Table 1 for more details on model formulation and demographic parameters, and Appendix S6 for equivalent plot calculated with alternative process noise-only likelihood functions.

or with process noise-only likelihood functions produced equivalent conclusions (compare Fig. 1 with Appendix S6).

Visually inspecting the fits for the four calibrated models revealed why the "Allometric N-history" model performed the best (Figs 2–4). Because model selection (Table 2) and relationships of demographic and uptake parameters (Fig. 1 and Appendix S6) were consistent between the process error-only and observation error-only models, we focus here only on observation error-only models. Cells that were previously N-replete and re-supplied with a single-nitrogen source showed up to 4 days of smooth nitrogen depletion (symbols in Fig. 2a and c), with gradual decrease in mean cell size (bars in Fig. 2a and c) and increase in population density (Fig. 2b and d). In contrast, previously N-deplete cells reared under the same nitrogen regime depleted all available nitrogen within 48 h (symbols in Fig. 3a and c), displaying an abrupt spike in mean cell size (bars in Fig. 3a and c) and a faster increase towards population carrying capacity (Fig. 3b and d). The same qualitative differences remained when cells were simultaneously supplied with both nitrate and ammonium: N-replete cells consistently displayed more regular transitions than N-deplete cells (compare Fig. 4a–c with Fig. 4d–f). Only the "Allometric N-history" model performed consistently well ($R^2_{allom\_N-hist} > 0 \cdot 89$) with both smooth and abrupt dynamics from N-replete and N-deplete cells respectively (dark blue line in Figs 2–4). The "Baseline" and "N-history" models performed well ($R^2_{baseline} > 0 \cdot 78$ and $R^2_{N-hist} > 0 \cdot 9$) only with smooth N-replete dynamics (yellow and orange lines respectively; Figs 2 and 4a–c), instead showing clear lack of fit from data collected for N-deplete cultures ($R^2_{baseline} > 0 \cdot 17$ and $R^2_{N-hist} > 0 \cdot 68$; Figs 3b,d and 4f). Conversely, the "Allometric" model showed mostly good fits for abrupt N-deplete cultures ($R^2_{allom} > 0 \cdot 83$; Figs 3 and 4d–f), but often failed to capture the smooth dynamics in N-replete cultures ($R^2_{allom} > 0 \cdot 46$; Figs 2b–d and 4c).

The explanation for the poor performance of the "Allometric" model with N-replete cells and of the "N-history" model with N-deplete cells lies in the observed mean cell sizes: N-deplete cells changed their size more suddenly than N-replete cells (compare bars in Figs 2a,c, and 4a against bars in Figs 3a,c, and 4d), mostly also recording higher peak values. The "Allometric" model can perform well with N-deplete cells because these rapid changes in cell size are indicative of imminent transitions in culture dynamics. However, this relationship between cell size and cell performances changed between N-replete and N-deplete cells. Consequently, forcing a single functional response for both N-deplete and N-replete cells (as assumed in the "Allometric" model) was inadequate and produced worse fits than the size-independent "baseline" and "N-history" models. This is the reason why the "Allometric N-history" model (assuming two different allometric relationship between N-replete and N-deplete cells) can combine the good performances of the "Allometric" model for N-deplete cells and of the "N-history" model for N-replete cells.

Overall, changes in mean cell size closely matched the transitions in medium nitrogen in the cultures: increasing cell size coincided with periods of high medium nitrogen, and decreasing cell size with periods of no available nitrogen (Figs 2a,c, 3a,c, and 4a,d). Thus, it is not surprising

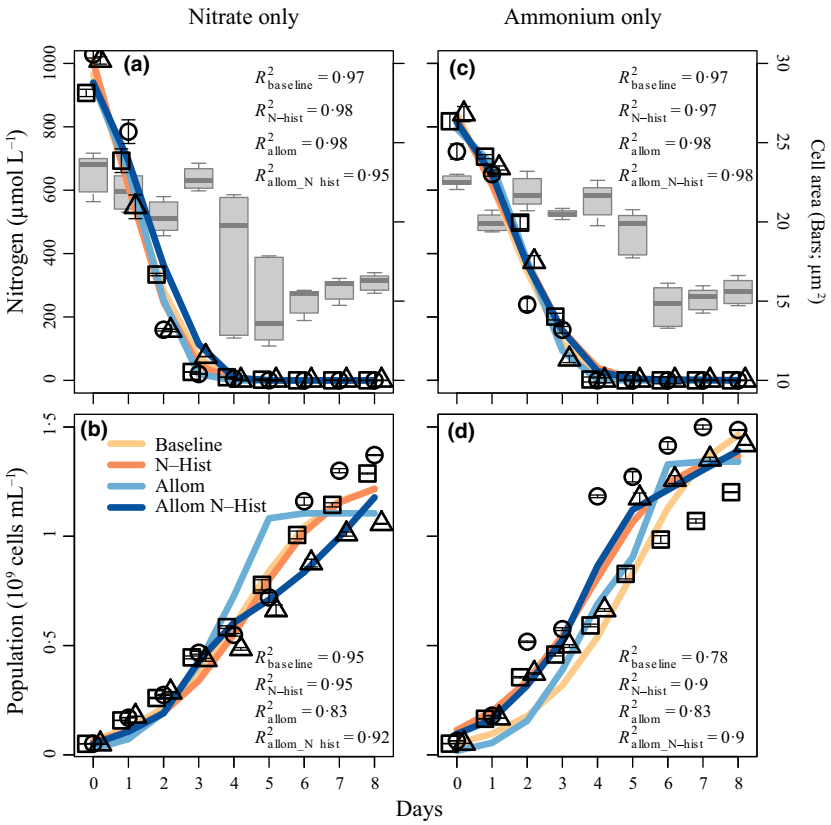

Fig. 2. Time series and model fits for nitrogen-replete culture dynamics grown with either nitrate (a, b) or ammonium (c, d) as the only nitrogen source. Plots show changes in medium nitrogen depletion (a, c) and population size (b, d) over the course of the experiments. Grey boxes represent daily estimates for optical proxy for mean population cell size (a, c). Different symbols represent the mean (±1 SE) among three replicate measurments for each day for each of the three independent replicate culture. Colour lines represent model goodness-of-fit for the four competing models calibrated with observation error-only likelihood functions (see Calibration section in Material and Methods). A coefficient of determination quantifies the goodness-of-fit for each competing model.

that observations on population mean cell size and model-inferred internal nitrogen quota from the best-fitting "Allometric N-history" model were highly correlated (Spearman's rho correlation: r_s = 0·8, S = 6048, P < 0·001, N = 57; Appendix S7). Interestingly, however, the relationship was consistent for both N-replete and N-deplete cells (Appendix S7).

High ammonium concentrations produced a temporary phase of slow or absent nitrate uptake (low nitrate depletion in the first 24 h in Fig. 4a,d). Most models captured this behaviour well, which indicates that the deterministic structure of the model was adequate to describe ammonium-induced inhibition of nitrate uptake for this species. The functional response calibrated with the best-fitting Allometric N-history model indicates a strong effect of ammonium on the nitrate uptake system: ammonium concentrations of 200 µM were sufficient to nearly fully inhibit the nitrate uptake system of a cell (see Appendix S8).

Discussion

Previous ecological studies have compared within-species trait variability with between-species variability. However, it has previously not been clear how or to what extent intraspecific trait variability influences population-dynamic and nutrient-uptake processes. The present analysis supported our hypothesis that nutrient utilization dynamics of *D. armatus* vary strongly with cell size and nutrient history. Specifically, larger cells recorded higher ammonium uptake rate, maximum specific growth rate and minimum internal nitrogen quota. Furthermore, rates of ammonium uptake were higher in cells recovering from N-depletion, while maximum cell growth rates increased with cell size more under N-replete than N-deplete conditions. Minimum cell quota increased with size under N-deplete conditions, but remained virtually constant under N-replete conditions. Finally, the positive relationship between mean cell size and (model-inferred) changes in internal nitrogen quota was consistent between N-replete and N-deplete cells across all experiments.

Our physiological understanding of the effect of N-stress in phytoplankton cells is consistent with the strong effects of mean cell size and previous N-history on phytoplankton nutrient utilization traits. For instance, our results demonstrate that larger cells show higher values for maximum cell growth rates (parameter μ_{inf}) under N-replete conditions. This is consistent with larger cells being at a more advanced stage of the cell division cycle (Hunter-Cevera *et al.* 2014). Conversely, maximum cell growth rates for N-deplete cells were independent of cell size. This is possibly because, when N availability inhibits the growth rate of the population, cell size decreases and photosynthetic energy is diverted and stored in the form of lipids or carbohydrates (Rodolfi *et al.* 2009; Mata, Martins & Caetano 2010). When small N-deplete cells are exposed to new nutrients, these energy stores can reactivate cell division at a rate that is temporarily enhanced and comparable to the growth rate of larger cells (Bittar *et al.* 2013). Moreover, rates for ammonium uptake were consistently higher for N-deplete than N-replete cells. This is likely because many

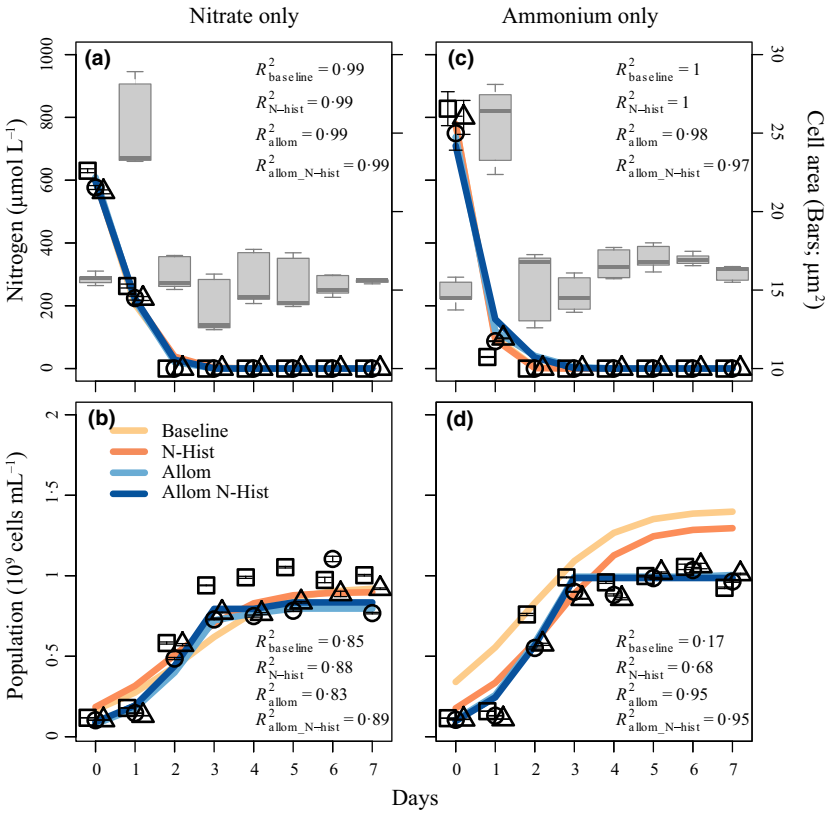

Fig. 3. Time series and model fits for nitrogen-deplete culture dynamics grown with either nitrate (a, b) or ammonium (c, d) as the only nitrogen source. Plots show changes in medium nitrogen depletion (a, c) and population size (b, d) over the course of the experiments. Grey boxes represent daily estimates for optical proxy for mean (a, c). Different symbols represent the mean (± 1 SE) among three replicate measurments for each day for each of the three independent replicate culture. Model fits were calculated using observation error-only likelihood functions. See legend for Fig. 2 for more information.

species are adapted to exploit new supplies of a limiting nutrient by taking up more than would be required to sustain immediate growth (Sinclair *et al.* 2006). However, enhanced N uptake is more common when cells are supplied with ammonium, and less frequent with nitrate (Cochlan & Harrison 1991). This is also because ammonium is easier to assimilate, as most amino acids are in the same oxidation state. In contrast, nitrate can be assimilated only after being first reduced to ammonium, by means of specialized enzymes (Dortch 1990; Crawford *et al.* 2000). Overall, our results show that using single species-specific parameter values (i.e. "Baseline model") leads to a substantial underestimation of a species' ability to divide (up to 43%), uptake ammonium (up to 65%) and nitrate (up to 37%), and to store nitrogen intracellularly (up to 64%), compared to accounting for variation due to cell size and N-history ("Allometric N-history model").

It is often assumed that within-species trait variability in phytoplankton species is negligible compared to between-species variability. However, this assumption is rarely tested. A way to estimate the relative importance of within-species sources of trait variation is to use information from published phytoplankton allometric relationships. We compared the range between minimum and maximum within-species trait values recorded here for each trait, against the standard deviation of the residuals in allometric scaling relationships across multiple species for the same trait. In this study, mean rates for nitrate uptake increased by up to 40%, while ammonium uptake, maximum growth rate and minimum internal nitrogen quota increased between half and one and a half orders of magnitude. These ranges were low (within one standard deviation of between-species residual variation) for nitrate uptake, but were substantially higher (by more than three standard deviations) for ammonium uptake, maximum growth rate and minimum nitrogen quota when compared to the residual standard deviations in interspecific allometric N-utilization traits for freshwater phytoplankton communities reported in Edwards *et al.* (2012). This indicates that for three of the four traits not accounting for phenotypic plasticity and intraspecific trait variability can lead to substantial uncertainty when calculating interspecific allometric relationships.

Overall, our findings are in agreement with the growing body of ecological literature highlighting the importance of phenotypic plasticity on species traits (Mommer *et al.* 2006; Violle et al. 2007). Phenotypic plasticity can provide an advantage to an individual by better adjusting to changes in abiotic conditions, while simultaneously decreasing interspecific competition by reducing niche overlap (Jung *et al.* 2010). In phytoplankton communities, cell size is influenced by nutrient regimes, geographic distribution, grazing risks and sinking velocity (Duarte, Agusti and Canfield 1990; Grover 1991; Maranon 2015). Similarly, plant communities occupying dynamic and unpredictable habitats, such as river floodplains, are dominated by species featuring wide phenotypic plasticity in traits determining gas exchange and submergence tolerance (Mommer *et al.* 2006; Jung *et al.* 2010). Another example is the common fruit fly *Drosophila melanogaster*, whose

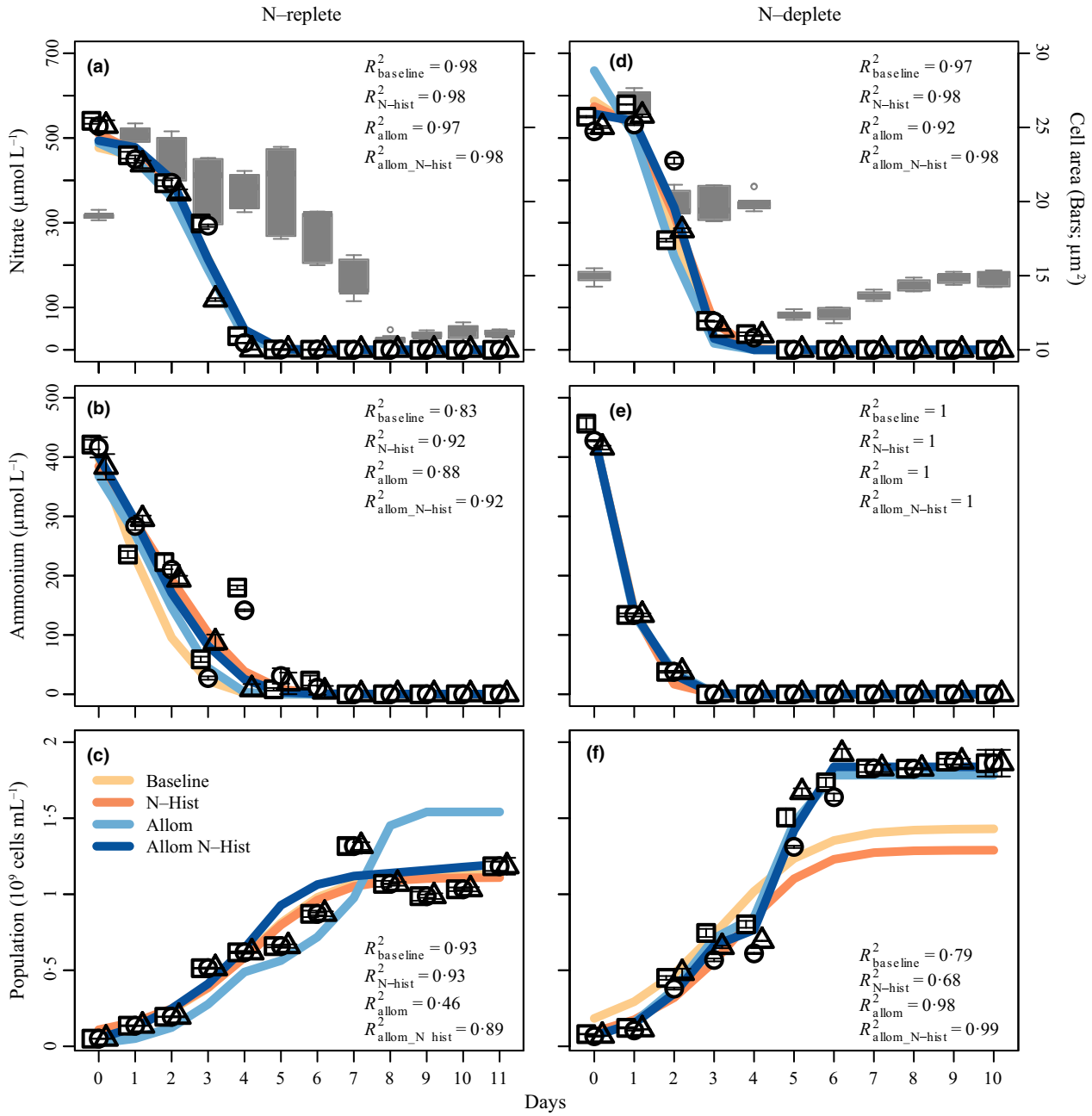

Fig. 4. Time series and model fits for nitrogen-replete (a–c) and nitrogen-deplete (d–f) cultures grown with both nitrate and ammonium as the only nitrogen source. Plots show changes in medium nitrogen depletion (a–b, d–e) and population size (c, f) over the course of the experiments. Grey boxes represent daily estimates for optical proxy for mean (a, d). Different symbols represent the mean (±1 SE) among three replicate measurments for each day for each of the three independent replicate culture. Model fits were calculated using observation error-only likelihood functions. See legend for Fig. 2 for more information.

ability to thrive at different temperatures has large intraspecific variability, with the expression of heat-shock proteins depending on previous thermal regimes experienced throughout the life history of the individual (Krebs & Feder 1997). Further examples of intraspecific trait plasticity include relationships between mean clutch size and exposure to predators for the freshwater crustacean *Daphnia pulex* (DeWitt 1998) and between development time and desiccation risk in the amphibian *Rana temporaria* (Merila, Laurila & Lindgren 2004).

In conclusion, our results show that intraspecific trait variability can play an important role in the population and nutrient-uptake dynamics of a species. Specifically, the nutrient utilization dynamics of the phytoplankton species *D. armatus* are functions of changes in mean cell size and previous nitrogen history. The importance of recognizing and quantifying trait plasticity in single species has become more urgent since a growing number of plant and animal studies use trait databases to investigate community patterns (Berg & Ellers 2010). Quantifying intraspecific trait

plasticity is complex and most trait databases often report only fixed species-specific values for each life-history trait (Vieira *et al*. 2006; Kleyer *et al*. 2008). Hence, it is important to recognize and distinguish between traits where interspecific variability is dominant, and traits where ignoring intraspecific trait plasticity will impair the explanatory power of trait-based analyses (Berg & Ellers 2010).

Acknowledgements

We are grateful to the North Queensland Algal Identification and Culturing Facility (NQAIF), in particular Stan Hudson and Florian Berner. We are grateful to the Ecological Modelling Research Group at James Cook University, especially Dr Loic Thibaut for comments on modelling techniques and R codes. Also, thanks to the High Performance Computing team at James Cook University. We thank Dr Lyndon Llewellyn, Dr Christian Lonborg and Dr Catia Carreira for helpful advice. Finally, we thank A/Prof A. Martiny and an anonymous reviewer for detailed and constructive comments on the manuscript. This research was supported by AIMS@JCU (aims.jcu.edu.au), the Australian Institute of Marine Science (www.aims.gov.au), the Advanced Manufacturing Cooperative Research Centre (Project 2.3.4) and James Cook University (www.jcu.edu.au). The authors declare no conflict of interest.

Data accessibility

The data associated with this article are publicly accessible in the Tropical Data Hub at http://dx.doi.org/10.4225/28/56A1BD8A2258D (Malerba, Connolly & Heimann, 2016b).

References

Aksnes, D.L. & Egge, J.K. (1991) A theoretical model for nutrient uptake in phytoplankton. *Marine Ecology Progress Series*, **70**, 65–72.

Albert, C.H., Grassein, F., Schurr, F.M., Vieilledent, G. & Violle, C. (2011) When and how should intraspecific variability be considered in trait-based plant ecology? *Perspectives in Plant Ecology Evolution and Systematics*, **13**, 217–225.

Albert, C.H., Thuiller, W., Yoccoz, N.G., Douzet, R., Aubert, S. & Lavorel, S. (2010) A multi-trait approach reveals the structure and the relative importance of intra- vs. interspecific variability in plant traits. *Functional Ecology*, **24**, 1192–1201.

Berg, M. & Ellers, J. (2010) Trait plasticity in species interactions: a driving force of community dynamics. *Evolutionary Ecology*, **24**, 617–629.

Berges, J.A. (1997) Minireview: Algal nitrate reductases. *European Journal of Phycology*, **32**, 3–8.

Bittar, T.B., Lin, Y.J., Sassano, L.R., Wheeler, B.J., Brown, S.L., Cochlan, W.P. & Johnson, Z.I. (2013) Carbon allocation under light and nitrogen resource gradients in two model marine phytoplankton. *Journal of Phycology*, **49**, 523–535.

Bolker, B. (2008) Dynamic models. *Ecological Models and Data in R* (ed. B. Bolker), pp. vii, 396. Princeton University Press, Princeton, NJ, USA.

Bower, C.E. & Holm-Hansen, T. (1980) A Salicylate-Hypochlorite method for determining ammonia in seawater. *Canadian Journal of Fisheries and Aquatic Sciences*, **37**, 794–798.

Chisholm, S.W. (1992) Phytoplankton size. *Primary Productivity and Biogeochemical Cycles in the sea* (eds P.G. Falkowski & A.D. Woodhead), pp. 213–237. Springer, Upton, New York, NY, USA.

Cochlan, W.P. & Harrison, P.J. (1991) Uptake of nitrate, ammonium, and urea by nitrogen-starved cultures of *Micromonas pusilla* (Prasinophyceae) - transient responses. *Journal of Phycology*, **27**, 673–679.

Collos, Y., Mornet, F., Sciandra, A., Waser, N., Larson, A. & Harrison, P.J. (1999) An optical method for the rapid measurement of micromolar concentrations of nitrate in marine phytoplankton cultures. *Journal of Applied Phycology*, **11**, 179–184.

Collos, Y., Vaquer, A., Bibent, B., Slawyk, G., Garcia, N. & Souchu, P. (1997) Variability in nitrate uptake kinetics of phytoplankton communities in a mediterranean coastal lagoon. *Estuarine Coastal and Shelf Science*, **44**, 369–375.

Collos, Y., Vaquer, A. & Souchu, P. (2005) Acclimation of nitrate uptake by phytoplankton to high substrate levels. *Journal of Phycology*, **41**, 466–478.

Crawford, N.M., Kahn, M.L., Leustek, T. & Long, S.R. (2000) Nitrogen and sulfur. *Biochemistry and Molecular Biology of Plants* (eds B.B. Buchanan, W. Gruissem & R.L. Jones), pp. 786–849. American Society of Plant Physiologists, Rockville, MD, USA.

Dassow, P.v., Chepurnov, V.A. & Armbrust, E.V. (2006) Relationships between growth rate, cell size, and induction of spermatogenesis in the centric diatom *Thalassiosira weissflogii* (Bacillariophyta). *Journal of Phycology*, **42**, 887–899.

De La Rocha, C.L., Terbruggen, A., Volker, C. & Hohn, S. (2010) Response to and recovery from nitrogen and silicon starvation in *Thalassiosira weissflogii*: Growth rates, nutrient uptake and C, Si and N content per cell. *Marine Ecology Progress Series*, **412**, 57–68.

DeWitt, T.J. (1998) Costs and limits of phenotypic plasticity: Tests with predator-induced morphology and life history in a freshwater snail. *Journal of Evolutionary Biology*, **11**, 465–480.

Dortch, Q. (1990) The interaction between ammonium and nitrate uptake in phytoplankton. *Marine Ecology Progress Series*, **61**, 183–201.

Droop, M.R. (1974) The nutrient status of algal cells in continuous culture. *Journal of the Marine Biological Association of the United Kingdom*, **54**, 825–855.

Duarte, C.M., Agusti, S. & Canfield, D.E. (1990) Size plasticity of freshwater phytoplankton - implications for community structure. *Limnology and Oceanography*, **35**, 1846–1851.

Edwards, K.F., Thomas, M.K., Klausmeier, C.A. & Litchman, E. (2012) Allometric scaling and taxonomic variation in nutrient utilization traits and maximum growth rate of phytoplankton. *Limnology and Oceanography*, **57**, 554–566.

Ellison, A.M. (2001) Interspecific and intraspecific variation in seed size and germination requirements of Sarracenia (*Sarraceniaceae*). *American Journal of Botany*, **88**, 429–437.

Fajardo, A. & Piper, F.I. (2011) Intraspecific trait variation and covariation in a widespread tree species (*Nothofagus pumilio*) in Southern Chile. *New Phytologist*, **189**, 259–271.

Falkowski, P.G., Barber, R.T. & Smetacek, V.V. (1998) Biogeochemical controls and feedbacks on ocean primary production. *Science*, **281**, 200–207.

Flynn, K.J. (1999) Nitrate transport and ammonium-nitrate interactions at high nitrate concentrations and low temperature. *Marine Ecology Progress Series*, **187**, 283–287.

Follows, M.J., Dutkiewicz, S., Grant, S. & Chisholm, S.W. (2007) Emergent biogeography of microbial communities in a model ocean. *Science*, **315**, 1843–1846.

Gelman, A. & Rubin, D.B. (1992) Inference from iterative simulation using multiple sequences. *Statistical Science*, **7**, 457–472.

Grover, J.P. (1990) Influence of cell size and shape on algal competitive ability. *Journal of Phycology*, **25**, 402–405.

Grover, J.P. (1991) Resource competition in a variable environment - phytoplankton growing according to the variable-internal-stores model. *American Naturalist*, **138**, 811–835.

Hall, B. (2008) *Laplacesdemon: An R Package for Bayesian Inference*.

L'Helguen, S., Maguer, J.-F. & Caradec, J. (2008) Inhibition kinetics of nitrate uptake by ammonium in size-fractionated oceanic phytoplankton communities: Implications for new production and f-ratio estimates. *Journal of Plankton Research*, **30**, 1179–1188.

Hilborn, R. & Mangel, M. (1997) *The Ecological Detective: Confronting Models With Data*. Princeton University Press, Princeton, NJ, USA.

Hooten, M.B. & Hobbs, N.T. (2015) A guide to bayesian model selection for ecologists. *Ecological Monographs*, **85**, 3–28.

Hunter-Cevera, K.R., Neubert, M.G., Solow, A.R., Olson, R.J., Shalapyonok, A. & Sosik, H.M. (2014) Diel size distributions reveal seasonal growth dynamics of a coastal phytoplankter. *Proceedings of the National Academy of Sciences of the United States of America*, **111**, 9852–9857.

Irwin, A.J., Finkel, Z.V., Schofield, O.M.E. & Falkowski, P.G. (2006) Scaling-up from nutrient physiology to the size-structure of phytoplankton communities. *Journal of Phytoplankton Research*, **28**, 459–471.

Shuter, B.J. (1978) Size-dependence of phosphorus and nitrogen subsistence quotas in unicellular micro-organisms. *Limnology and Oceanography*, **23**, 1248–1255.

Jung, V., Violle, C., Mondy, C., Hoffmann, L. & Muller, S. (2010) Intraspecific variability and trait-based community assembly. *Journal of Ecology*, **98**, 1134–1140.

Kleyer, M., Bekker, R.M., Knevel, I.C., Bakker, J.P., Thompson, K., Sonnenschein, M., Poschlod, P., Van Groenendael, J.M., Klimeš, L., Klimešová, J., Klotz, S., Rusch, G.M., Hermy, M., Adriaens, D., Boedeltje, G., Bossuyt, B., Dannemann, A., Endels, P., Götzenberger, L., Hodgson, J.G., Jackel, A.K., Kühn, I., Kunzmann, D., Ozinga, W.A., Römermann, C., Stadler, M., Schlegelmilch, J., Steendam, H.J., Tackenberg, O., Wilmann, B., Cornelissen, J.H.C., Eriksson, O., Garnier, E. & Peco, B. (2008) The LEDA traitbase: a database of life-history traits of the northwest european flora. *Journal of Ecology*, **96**, 1266–1274.

Krebs, R.A. & Feder, M.E. (1997) Natural variation in the expression of the heat-shock protein HSP70 in a population of *Drosophila melanogaster* and its correlation with tolerance of ecologically relevant thermal stress. *Evolution*, **51**, 173–179.

Lanoul, A., Coleman, T. & Asher, S.A. (2002) UV resonance raman spectroscopic detection of nitrate and nitrite in wastewater treatment processes. *Analytical Chemistry*, **74**, 1458–1461.

Lavorel, S., McIntyre, S., Landsberg, J. & Forbes, T.D. (1997) Plant functional classifications: from general groups to specific groups based on response to disturbance. *Trends in Ecology & Evolution*, **12**, 474–478.

Litchman, E. & Klausmeier, C.A. (2008) Trait-based community ecology of phytoplankton. *Annual Review of Ecology Evolution and Systematics*, **39**, 615–639.

Litchman, E., Klausmeier, C.A., Schofield, O.M. & Falkowski, P.G. (2007) The role of functional traits and trade-offs in structuring phytoplankton communities: scaling from cellular to ecosystem level. *Ecology Letters*, **10**, 1170–1181.

Lyczkowski, E.R. & Karp-Boss, L. (2014) Allelopathic effects of *Alexandrium fundyense* (Dinophyceae) on *Thalassiosira* cf. *gravida* (Bacillariophyceae): a matter of size. *Journal of Phycology*, **50**, 376–387.

Malerba, M.E., Connolly, S.R. & Heimann, K. (2012) Nitrate-nitrite dynamics and phytoplankton growth: Formulation and experimental evaluation of a dynamic model. *Limnology and Oceanography*, **57**, 1555–1571.

Malerba, M.E., Connolly, S.R. & Heimann, K. (2015) An experimentally validated nitrate-ammonium-phytoplankton model including effects of starvation length and ammonium inhibition on nitrate uptake. *Ecological Modelling*, **317**, 30–40.

Malerba, M.E., Connolly, S.R. & Heimann, K. (2016a) Standard flow cytometry as a rapid and non-destructive proxy for cell nitrogen quota. *Journal of Applied Phycology*, **28**, 1085–1095.

Malerba, M.E., Connolly, S.R. & Heimann, K. (2016b) Nitrate-ammonium utilisation for the green alga species *Desmodesmus armatus* reared in laboratory batch culture conditions. James Cook University. [Data files] http://dx.doi.org/10.4225/28/56A1BD8A2258D

Maranon, E. (2015) Cell size as a key determinant of phytoplankton metabolism and community structure. *Annual Review of Marine Science*, **7**(7), 241–264.

Maranon, E., Cermeno, P., Lopez-Sandoval, D.C., Rodriguez-Ramos, T., Sobrino, C., Huete-Ortega, M., Blanco, J.M. & Rodriguez, J. (2013) Unimodal size scaling of phytoplankton growth and the size dependence of nutrient uptake and use. *Ecology Letters*, **16**, 371–379.

Mata, T.M., Martins, A.A. & Caetano, N.S. (2010) Microalgae for biodiesel production and other applications: A review. *Renewable & Sustainable Energy Reviews*, **14**, 217–232.

McGill, B.J., Enquist, B.J., Weiher, E. & Westoby, M. (2006) Rebuilding community ecology from functional traits. *Trends in Ecology & Evolution*, **21**, 178–185.

Merila, J., Laurila, A. & Lindgren, B. (2004) Variation in the degree and costs of adaptive phenotypic plasticity among *Rana temporaria* populations. *Journal of Evolutionary Biology*, **17**, 1132–1140.

Mommer, L., Lenssen, J.P.M., Huber, H., Visser, E.J.W. & De Kroon, H. (2006) Ecophysiological determinants of plant performance under flooding: a comparative study of seven plant families. *Journal of Ecology*, **94**, 1117–1129.

Mullaney, P.F., Dilla, M.A.V. & Coulter, J.R. (1969) Cell sizing: a light scattering photometer for rapid volume determination. *Review of Scientific Instruments*, **40**, 1029–1032.

Nichols, H.W. (1973) Growth media - freshwater. *Handbook of Phycological Methods* (ed. J. Stein), pp. 448. Cambridge University Press, Cambridge, UK.

R Core Team (2015) *R: A Language and Environment for Statistical Computing*. R foundation for statistical computing, Vienna, Austria. http://www.R-project.Org/.

Rodolfi, L., Zittelli, G.C., Bassi, N., Padovani, G., Biondi, N., Bonini, G. & Tredici, M.R. (2009) Microalgae for oil: Strain selection, induction of lipid synthesis and outdoor mass cultivation in a low-cost photobioreactor. *Biotechnology and Bioengineering*, **102**, 100–112.

Shapiro, H.M. (2005) Parameters and probes. *Practical Flow Cytometry* (ed. H.M. Shapiro), pp. 736. Wiley-Liss, New Jersey.

Sharpless, T.K. & Melamed, M.R. (1976) Estimation of cell size from pulse shape in flow cytofluorometry. *Journal of Histochemistry Cytochemistry*, **24**, 257–264.

Sharpless, T.K., Traganos, F., Darzynkiewicz, Z. & Malemed, M.R. (1975) Flow cytofluorimetry: discrimination between single cells and cell aggregates by direct size measurements. *Acta Cytologica*, **19**, 577–581.

Sinclair, G.A., Kamykowski, D., Milligan, E. & Schaeffer, B. (2006) Nitrate uptake by *Karenia brevis*. I. Influences of prior environmental exposure and biochemical state on diel uptake of nitrate. *Marine Ecology Progress Series*, **328**, 117–124.

Spiegelhalter, D.J., Best, N., Carlin, B.P. & Linde, A.V.D. (2002) Bayesian measures of model complexity and fit. *Journal of the Royal Statistical Society B*, **64**, 583–640.

Stolte, W. & Riegman, R. (1995) Effect of phytoplankton cell size on transientstate nitrate and ammonium uptake kinetics. *Microbiology*, **141**, 1221–1229.

Stolte, W. & Riegman, R. (1996) A model approach for size-selective competition of marine phytoplankton for fluctuating nitrate and ammonium. *Journal of Phycology*, **32**, 732–740.

Syrett, P.J. & Morris, I. (1963) The inhibition of nitrate assimilation by ammonium in chlorella. *Biochimica et Biophysica Acta*, **67**, 566–575.

Veldhuis, M.J.W. & Kraay, G.W. (2000) Application of flow cytometry in marine phytoplankton research: Current applications and future perspectives. *Scientia Marina*, **64**, 121–134.

Vieira, N., Poff, N., LeRoy, C., Moulton, S., Koski, M. & Kondratieff, C. (2006) A database of Lotic invertebrate traits for North America: US geological survey data series 187.

Violle, C., Navas, M.-L., Vile, D., Kazakou, E., Fortunel, C., Hummel, I. & Garnier, E. (2007) Let the concept of trait be functional!. *Oikos*, **116**, 882–892.

Wirtz, K.W. (2011) Non-uniform scaling in phytoplankton growth rate due to intracellular light and CO_2 decline. *Journal of Plankton Research*, **33**, 1325–1341.

Received 5 November 2015; accepted 21 February 2016
Handling Editor: Shawn Leroux

Supporting Information

Additional Supporting Information may be found online in the supporting information tab for this article:

Appendix S1. Relationship per-capita nitrogen uptake and medium nitrogen.

Appendix S2. Details on laboratory procedures.

Appendix S3. Experimental design.

Appendix S4. Relationship cell size and forward scatter.

Appendix S5. Phenomenological models of observed rates.

Appendix S6. Demographic parameters with process noise-only likelihood functions.

Appendix S7. Correlation between internal quota and cell size.

Appendix S8. Ammonium inhibition on nitrate uptake.

